A Theoretical Study of the S + C_3H Reaction: Potential Energy Surfaces

J. R. Flores* and F. J. Gómez

Departamento de Química Física, Facultad de Ciencias, Universidad de Vigo, Lagoas-Marcosende, 36200-Vigo (Pontevedra), Spain

Received: April 23, 2001; In Final Form: July 26, 2001

A theoretical study of the potential energy surfaces of the S + *c*-C_3H and S + *l*-C_3H reactions has been carried out. The most important local minima and saddle points have been located at the B3LYP/6-311G** and QCISD/6-311G** levels, whereas a G2-style method based on QCISD(T)/6-311+G(3df,2p) electronic energies has been used to calculate accurate relative energies. The lowest lying state is a nearly linear SCCCH ($^2A'$) species, but a SC_3H ($^2A'$) species, with a cyclic C_3H group attached to sulfur, is 17.1 kcal/mol higher in energy. The reaction appears to be exothermic for the production of SC_3 ($^1\Sigma^+$) + H and SC ($^1\Sigma^+$) + C_2H ($^2\Sigma^+$). The reaction mechanisms are rather involved for the products may be generated from SCCCH ($^2A'$) or imply some other intermediates. The energy profiles for the interaction of sulfur with both *l*-C_3H and *c*-C_3H through the lowest lying doublet and quartet states have also been computed by means of the CASSCF method. We have found at least two neatly attractive electronic states in each case. The vertical energy gap between the ground and the lowest-lying states has been determined through the MRCI method for each reaction intermediate. The S + C_3H reaction could indeed be a source of SC_3 ($^1\Sigma^+$), but its efficiency would depend on the SC_3 + H/SC + C_2H branching ratio.

I. Introduction

The sulfur−carbon chains SC_n ($n = 1-3$ and 5) have received considerable theoretical and experimental attention, partly for their astrophysical significance.[1−7] The groups of Lovas et al.,[2] Oshima et al.,[3] Hirahara et al.,[4] Kasai et al.,[5] and Saito et al.[6] have recorded the Fourier transform microwave spectra of SC_n, $n = \{2, 3, \text{and } 5\}$ generated in Fabry−Perot cavities. Vala and co-workers[7] have produced (SC_n and SC_nS, $n = 1-5$) by pulsed laser ablation of carbon/sulfur mixtures and recorded the Fourier transform infrared absorption spectra in an Ar matrix. Maier and co-workers have also detected SC_3 in Ar matrixes by infrared absorption spectroscopy.[8] The most recent theoretical work should also be cited. Lee[9] has studied the linear SC_n systems $n = 2-9$ through a (density functional) BLYP method, whereas Vala and co-workers[7] have accompanied their experimental work with B3LYP and MP2 (second-order Möller−Plesset) computations. The ionization potential and proton affinity of the SC_n molecules $n = \{2 \text{ and } 3\}$ have been computed by Maclagan and Sudkeaw.[10] Peeso et al.[11] have studied singlet and triplet linear states of SC_3 at the MP2/DZP level. Murakami[12] has computed vibrational frequencies, rotational constants, and dipole moments of the ground states of SC_n, $n = 1-3$. Botschwina and co-workers have made a detailed theoretical study of SC_3, which provides values for a number of spectroscopic properties.[13]

The most cited mechanisms for the astrophysical generation of SC_n involve ion−molecule reactions of the type

$$S^+ + C_2H_2 \rightarrow HC_2S^+ + H$$

followed by dissociative recombination steps

$$HC_2S^+ + e^- \rightarrow SC_2 + H$$

However, this kind of mechanism is not very satisfactory either for circumstellar envelopes or dark clouds; in fact, the critical role played by neutral−neutral reactions has been strongly advocated.[14,15] Vala and co-workers have also concluded that neutral−neutral reactions are responsible for the generation of the SC_n chains in their laser ablation experiments.[7]

The S + C_2H reaction has been proposed to be important in the production of SC_2,[14,15] although the opposite proposal has also been raised by Turner et al., who based their views in the modeling of small translucent clouds.[16] A recent theoretical study suggests that this reaction is rather fast and should produce almost exclusively SC_2 + H.[17] It has been argued that SC_3 could be generated by the following reactions:[14,15]

$$CS + C_2H \rightarrow C_3S + H$$

$$S + C_3H \rightarrow C_3S + H$$

Unfortunately the rate coefficients of these reactions or even the products are unknown. For this reason, we have made a theoretical study of the SC_3H system, which will be a first step of a dynamical study.

II. Computational Details

The local minima and transition states have been determined, and the vibrational frequencies have been computed at the B3LYP/6-311G**[18] level. The resulting geometries have been refined by means of QCISD/6-311G**[19,20] optimizations, although no second derivatives were computed at this level. In the case of a few transition states, we have employed QCISD/6-31G** vibrational frequencies instead of the B3LYP/6-311G** ones, which were considered more reliable, although the geometries were still refined at the QCISD/6-311G** level. The role of the transition structures in the dynamics has been checked by means of the intrinsic reaction coordinate method[21] in combination with the B3LYP/6-311G** level where neces-

* To whom correspondence should be addressed. E-mail: flores@uvigo.es.

10.1021/jp011532k CCC: $20.00
Published on Web 10/23/2001

sary. For the sake of obtaining accurate relative energies, we have used a Gaussian-style method that is closely related to the G2(QCI) approach.[22] This method has the following steps:

(1) Vibrational frequencies are scaled by a factor of 0.96 (B3LYP/6-311G**) or 0.95 (QCISD/6-31G**). This factor was determined by comparison of the computed values with the known experimental frequencies of ethylene, acetylene (C−H and C−C stretch), and also SC.[23]

(2) Electronic energies are determined at the QCISD(T)/6-311+G(3df,2p) level using the QCISD/6-311G** geometries (i.e., at the QCISD(T)/6-311+G(3df,2p)//QCISD/6-311G** level).

(3) The so-called high-level correction is defined as in the G2(QCI) approach as HLC= $-Bn_\alpha - An_\beta$, where n_α and n_β are the number of alpha and beta valence electrons ($n_\alpha \geq n_\beta$). *B* was given the original G2(QCI) value, and *A* was determined by minimization of the difference between the experimental[24] and theoretical values of $E = D_0(C_2H_2 \rightarrow 2CH) + {}^3/_2 D_0(C_2H_4 \rightarrow 2CH_2(^2B_1)) + D_0(SC \rightarrow S + C) + D_0(CH_2(^2B_1) \rightarrow C + 2H)/2$.

In the choice of these methods, we have valued the accuracy of the scaled B3LYP frequencies in the case of SC_3 ($^1\Sigma^+$)[7] and the fact that the QCISD method may remove the spin contamination of the reference wave function quite efficiently. The procedure for determining the HLC is expected to give better results than the standard one in the present case, for only the molecules with bonds that are relevant to the present case contribute to the value of *A*. The computations have been carried out with the Gaussian 94[25] and Gaussian 98[26] packages. We have also used the MOLPRO package[27] to perform CASSCF (complete active space SCF) computations,[28] which will be described in the next section. These computations have been necessary to study the interaction of ground-state sulfur with linear and cyclic C_3H (noted as *c*-C_3H and *l*-C_3H respectively) and to determine the energy gaps between the lowest-lying electronic states of some reaction intermediates.

III. Potential Energy Surfaces of the SC_3H System

III.1. Local Minima. The optimized geometries for the minima and saddle point structures on the potential energy surface (PES) of the lowest doublet state are given in Figure 1, parts a and b. Absolute and relative energies are presented in Table 1; vibrational frequencies and other details are available from the authors upon request.

The most stable form of SC_3H is SCCCH($^2\Pi$), this electronic term breaks into two components (Renner−Teller effect), namely, $^2A'$ and $^2A''$. The geometry optimizations of the latter electronic state led to a linear geometry, whereas those of the $^2A'$ state gave a planar structure, (which will be noted as M1), with a ∠SCC angle of about 155.5°. Note the ∠CCC angle and, specially, the ∠CCH angle are very close to 180°. The S−C bond length is only slightly larger than that of SC ($^1\Sigma^+$) (1.546 Å), the C_2-C_3 and C_3-C_4 distances are close to the C−C lengths of ethylene (1.340 Å) and acetylene (1.211 Å), respectively, and the C−H distance is almost coincident with that of acetylene (1.067 Å; all reference bond lengths are computed at the QCISD/6-311G** level). It must be noted that both McCarthy et al.[29] and Hirahara et al.[30] have found the minimum to be a linear structure in their microwave experiments, the electronic level being $^2\Pi_{1/2}$. However, the ab initio computations of McCarthy et al.[29] also indicate that the minimum is a nonlinear structure. Our computed difference between the linear and nonlinear configurations is only 0.12 kcal/mol (QCISD(T)/6-311+G(3df,2p)//QCISD/6-311G**). It has already been pointed out by McCarthy and co-workers[29] that inclusion of the spin−orbit coupling might be indispensable to obtain a linear geometry; this aspect will be the subject of our future work. We would also add that the significant degree of spin-contamination of the reference UHF/6-311G** wave function $\langle S^2 \rangle = 1.4$ is probably not the reason of the appearance of a nonlinear minimum. The B3LYP wave functions are almost spin-pure, and the corresponding levels (B3LYP/6-31G**, 6-311G**, 6-311+G**) behave the same way, i.e., give a nonlinear geometry. On the other hand, we have made a geometry optimization at the RHF-RCCSD(T)/cc-pVDZ level[31] which has also produced a bent geometry,[32] the corresponding wave functions being virtually spin-pure. The spin polarization effect does not appear to cause much trouble in the computation of the relative energy of this species. For instance, the M2-M1 energy gap is 17.8 kcal/mol at the QCISD/6-311G**//QCISD/6-311G**+ZPVE level, whereas the RHF-RCCSD/6-311G**//QCISD/6-311G**+ZPVE value is 19.4 kcal/mol; species M2 (to be described immediately) has a virtually spin pure UHF/6-311G** wave function ($\langle S^2 \rangle = 0.775$ au).

The Mulliken population analysis does not fully support Hirahara et al.'s conclusion that the electronic structure is a superposition of two valence structures,[30] namely, S=C=C=Ć−H and S=Ć−C≡C−H. For instance, the C−C and S−C overlap populations are 0.406 e (C_3-C_4), −0.126 e (C_2-C_3) and 0.953 e ($S-C_2$) at the QCISD/6-311G** level (all of the population data given in the following discussions correspond to this computational level and are of Mulliken type). This electronic structure is more consistent with that of (ground state) SC_3($^1\Sigma^+$), which has two triple terminal S−C and C−C bonds[33] or with the second valence structure proposed by Hirahara. C_2 bears most of the spin density (0.579 e), but the sulfur value is not negligible (0.242e). Although C_4 also presents an important contribution (0.417 e), it is partly the result of the spin polarization of the C_3-C_4 bond (C_3 appears to have −0.223 e). As in the case of SC_3($^1\Sigma^+$), the electron delocalization along the carbon chain may explain the short C_2-C_3 distance. We have performed MRCI computations on M1 and on the other local minima of the doublet PES in order to estimate the energy differences of the lowest lying doublet and quartet states with respect to the ground state. The $^2A''$ state lies only 7.0 kcal/mol above, but the lowest quartet states are much farther away, (see Table 2).

There is a minimum with a C_3 ring, corresponding to a $^2A'$ state with the following leading electron configuration [...3a″^{2}14a′^{2}15a′^{1}], which will be noted as M2. It is 17.1 kcal/mol higher in energy than M1. The S−C distance is still close to that of a double bond (d(SC) = 1.618 Å in thioformaldehyde), whereas the C−C distances are average between the typical values of double and single bonds (1.340 Å in ethylene and 1.532 Å in ethane). The C−H distance is very close to that of ethylene (1.088 Å). The population analysis indicates that the unpaired electron is located mainly at sulfur (0.563 e), but C_2 also has a sizable spin-density (0.302 e). The dominant valence structure has double S−C and C_2-C_4 bonds and one unpaired electron located mainly at sulfur, even though other valence structures, which locate the unpaired electron at C_2, also contribute significantly. The $^2A'-{}^2A''$, $^2A'-{}^4A''$, and $^2A'-{}^4A'$ energy gaps are much wider than in M1 (see Table 2); the lowest quartet states $^4A'$ and $^4A''$ lie only slightly below the reactants.

Structure M3 is also a minimum corresponding to the $^2A'$ electronic state and has a dominant [...3a″^{2}14a′^{2}15a′^{1}] electron configuration. The S−C distance is average between that of thioformaldehyde and methanethiol (d(SC) = 1.618 and 1.821

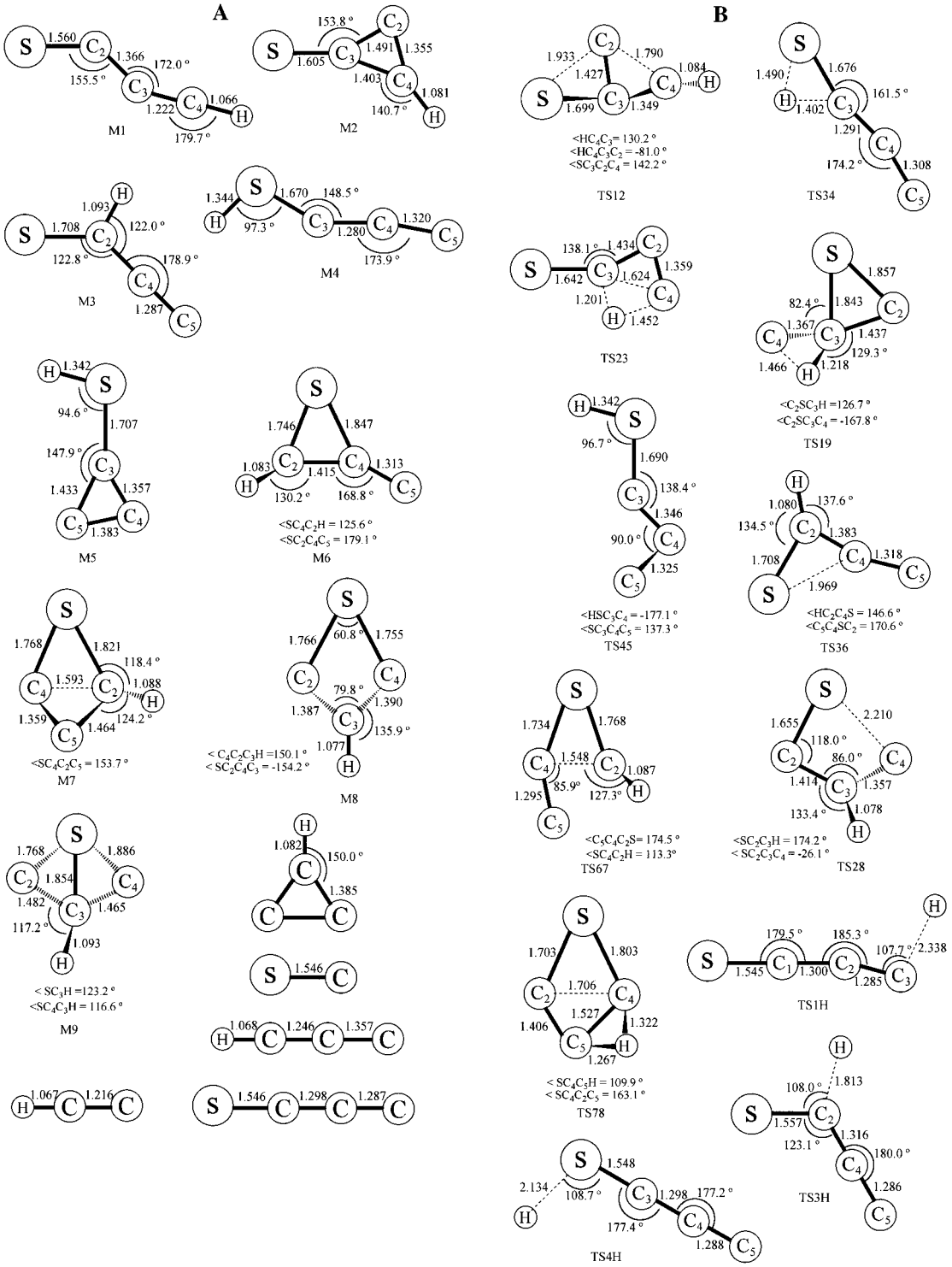

Figure 1. (A) QCISD/6-311G** optimized geometries for the local minima, reactants, and products. Bond distances are given in angstroms and angles are given in degrees. The electronic states of reactants and products are *c*-$C_3H(^2B_2)$, *l*-$C_3H(^2A)$, $SC(^1\Sigma^+)$, $SC_3(^1\Sigma^+)$, and $C_2H(^2\Sigma^+)$. (B) QCISD/6-311G** optimized geometries for the saddle points (angstroms and degrees).

Å respectively). The C_2-C_4 distance is almost coincident with that of ethylene, whereas the C_4-C_5 is larger than that of acetylene or $C_2H(^2\Sigma^+)$ (d(CC) = 1.216 Å), but still shorter than that of $C_2H(^2A)$ (d(CC) = 1.297 Å; the latter state is about 9.0 kcal/mol higher in energy at the QCISD/6-311G** level and gives rise to $^2A'$ and $^2A''$ components in planar geometries). The population analysis indicates that the unpaired electron is very neatly localized on sulfur (1.042 e); the C_2-C_4 and C_4-C_5 overlap populations are 0.362 e and 0.896 e, respectively. There is an excited $^2A''$ state lying only 11.3 kcal/mol above (see Table 2), but the lowest quartet states $^4A'$ and $^4A''$ are much higher in energy (54.7 and 47.4 kcal/mol respectively). We could even reach a minimum on the PES of the $^2A''$ state by constraining the search to planar geometries; however, its existence could not be confirmed due to wave function instabilities and convergence difficulties. It must be noted that this $^2A''$ "planar minimum" is still 9.2 kcal/mol higher in energy than M3 at the B3LYP/6-311G** level.

The next minimum, noted as M4, is very close in energy to M3 for it lies only 2.0 kcal/mol above. It corresponds to a $^2A'$

TABLE 1: Absolute and Relative Energies in Hartrees and kcal/mol, Respectively, for the States Considered in This Work

species	QCISD(T)[a]	ZPVE[b]	Δ[c]
$S(^3P) + C_3H(^2B_2)$	−512.10644	0.01835	0.0
$S(^3P) + C_3H(^2\Pi)$	−512.10254	0.02142	4.5
$SC(^1\Sigma^+) + C_2H(^2\Sigma^+)$	−512.15619	0.01642	−35.5
$SC_3(^1\Sigma^+) + H(^2S)$	−511.17299	0.01253	−48.4
$SC_2(^3\Sigma^-) + CH(^2\Pi)$	−512.02999	0.01297	44.8
$SC(^3\Pi) + C_2H(^2\Sigma^+)$	−512.02968	0.01599	46.8
$SC(^1\Sigma^+) + C_2H(^4A')$	−512.01073	0.01494	58.1
$M1(^2A')$	−512.28835	0.02027	−116.0
$M2(^2A')$	−512.26304	0.02223	−98.9
$M3(^2A')$	−512.21716	0.02173	−70.5
$M4(^2A')$	−512.21145	0.01908	−68.5
$M5(^2A)$	−512.20777	0.01907	−66.2
$M6(^2A)$	−512.18486	0.02017	−51.2
$M7(^2A)$	−512.18477	0.02043	−50.9
$M8(^2A)$	−512.22260	0.02163	−73.9
$M9(^2A)$	−512.14564	0.01982	−26.8
TS12	−512.15488	0.01857	−33.3
TS23	−512.16518	0.01698	−40.8
TS34	−512.16079	0.01537	−39.1
TS19	−512.10263	0.01614	−2.1
TS45	−512.17294	0.01814	−45.0
TS36	−512.18267	0.01918	−50.4
TS67	−512.17318	0.02005	−43.9
TS78	−512.12350	0.01517	−15.8
TS28	−512.20972	0.02058	−66.5
TS1H	−512.17122	0.01261[d]	−47.3
TS3H	−512.15881	0.01342[d]	−39.0
TS4H	−512.16667	0.01281	−44.4
$M1Q(^4A')$	−512.20199	0.01903	−59.4
$M2Q(^4A)$	−512.14978	0.02026	−25.8
$M3Q(^4A'')$	−512.15863	0.02047	−31.3
$M4Q(^4A')$	−512.14658	0.01838	−25.0
$M7Q(^4A'')$	−512.14952	0.02060	−25.5
$M8Q(^4A')$	−512.15739	0.02137	−29.9
$M10Q(^4A'')$	−512.15147	0.02092	−26.5
TS12Q	−512.14110	0.01827	−21.6

[a] The 6-311+G(3df.2p) basis and the QCISD/6-311G** geometry were employed. [b] Computed at the B3LYP/6-311G** level and scaled by 0.96, except for TS1H and TS3H. [c] $HLC = -0.00019n_\alpha - 0.005376n_\beta$. [d] Computed at the QCISD/6-31G** level and scaled by 0.95.

TABLE 2: Electronic Energy Gaps (kcal/mol) between the Ground State and the Lowest-Lying Doublet and Quartet States Computed at the Geometries of the Doublet Local Minima

local minimum	doublet	quartet	
M1[a]	7.0 ($^2A''$)	77.4 ($^4A'$)	77.0 ($^4A''$)
M2[a]	44.5 ($^2A''$)	91.3 ($^4A'$)	93.1 ($^4A''$)
M3[a]	11.3 ($^2A''$)	54.6 ($^4A'$)	47.4 ($^4A''$)
M4[a]	18.4 ($^2A''$)	76.1 ($^4A'$)	86.5 ($^4A''$)
M5[a]	78.2 ($^2A''$)	139.5 ($^4A'$)	83.4 ($^4A''$)
M6[b]	35.8 (^2A)	38.0 (^4A)	
M7[b]	30.2 (^2A)	66.5 (^4A)	
M8[b]	58.0 (^2A)	80.5 (^4A)	
M9[b]	17.4 (^2A)	46.4 (^4A)	

[a] MRCI including Davidson correction with an active space of [14a′15a′3a″4a″] for five electrons and a state-averaged $^2A'-^2A''-{}^4A'-{}^4A''$ CASSCF wave function (equal weights), in combination with the 6-311G** basis set. [b] Same with [17a−20a] for three electrons and a state-averaged $^2A-^2A-{}^4A$ wave function.

electronic state with the following electron configuration [. .14a′^{2}3a″^{2}15a′^{1}]. The S−H bond length is quite close to that of methanethiol (1.335 Å) but the S−C distance is much shorter (d(SC) = 1.821 Å in methanethiol), being not far from that of thioformaldehyde (d(SC) = 1.618 Å). Both C−C bonds can be considered average between double and triple, but the one closer to sulfur is shorter, in contrast with structure M1. Although M4 is planar, the lowest vibrational frequency, which corresponds to a HSCC torsional mode, is only 146 cm^{-1}. The unpaired electron is shared almost equally by C_3 and C_5 (0.607 e and 0.555 e, respectively), although the Fermi contact coupling parameter corresponding to $^{13}C_3$ (0.134 au) is much larger than the one of the terminal carbon (0.016 au), probably as a result of the sizable deviation of the ∠<SCC angle from 180°. The spin density of the terminal carbon resides in an in-plane B orbital centered on the terminal carbon. The $^2A''-^2A'$ energy gap is rather small 18.4 kcal/mol, but the $^2A''-^4A'$ and $^2A''-{}^4A''$ gaps are much wider (76.1 and 86.5 kcal/mol respectively).

We could also find another thiol, namely M5, which is only 2.3 kcal/mol higher in energy than M4. The electronic state is $^2A'$, and the leading electron configuration is [. .14a′^{2}3a″^{2}15a′^{1}], as in M4. It is interesting that the $^2A''-^2A'$ energy gap (78.2 kcal/mol) is much wider than in M4; the lowest quartet state is still higher in energy (the corresponding energy gap $^2A''-^4A''$ is 83.4 kcal/mol). The spin density is distributed among all carbon atoms, although C_4 has the largest population 0.543 e. Note that the H−S and S−C distances are quite similar to those of M4.

We have also found other high-lying species, namely, M6, M7, M8, and M9. Structure M6 has a SC_2 ring with hydrogen and a carbon atom bonded to the ring carbon atoms. The S−C bonds are somewhat longer and shorter than in methanethiol, and the C_2-C_4 distance is somewhat larger than that of a double bond. The spin density is localized mainly on the carbon atom bonded to hydrogen (0.803 e). Species M7 has a SC_3 ring. The C_4-C_5 and C_2-C_5 Mulliken overlap populations (0.804 e and 0.590 e) are consistent with the bond lengths. The unpaired electron is centered primarily on C_4 (0.764 e), but C_2 also bears a rather high spin density (0.538 e). M8 has also a four-membered ring. The Mulliken population analysis indicates that there is not a C_2-C_4 bond and that the unpaired electron is localized mainly on C_2 and C_4. It has a nearly symmetric C_s structure at the QCISD/6-311G** level, although the B3LYP/6-311G** optimization gave a strictly symmetric one.

The last minimum we were able to locate, M9, is a rather unusual SC_4 cycle. It is so high in energy that it is probably not important from the point of view of the reaction dynamics, but it has an interesting electronic structure. There is a rather low vibrational frequency (207 cm^{-1}) which corresponds to C_2SC_4 asymmetric stretching normal mode, but the next frequency in increasing order is relatively high (525 cm^{-1}) and corresponds to a CCC wagging mode. It must be pointed out that the B3LYP/6-311G** method leads to a symmetric C_s structure, whereas the QCISD/6-311G** approach leads to a nonsymmetric structure. As in the case of M8, this is probably the result of symmetry breaking effects,[34] particularly, the lowest $^2A'$ and $^2A''$ states interact strongly enough in nonsymmetric geometries to produce two equivalent nonsymmetric minima (doublet instability). We located a C_s-constrained minimum ($^2A''$) which is only 1.1 kcal/mol higher in energy than the nonsymmetric one at the QCISD/6-311G** level. As is often the case, it is very difficult to establish whether this species is truly symmetric or not, for this would require, for instance, large-scale MRCI-type computations. Given that M9 is the highest-lying species and probably has no influence in the dynamics of the reactions mentioned in the Introduction, we did not make any additional computation. Note that, although the $S-C_2$ and $S-C_4$ bond lengths are quite different, the C−C distances are very close; the structural asymmetry can be attributed mainly to a small rotation of the C_3H group about the C−H bond. The unpaired electron is localized mainly on C_4 (0.808 e), but C_2

has also a sizable spin density (0.293 e). The electronic structure can be viewed as the superposition of two valence structures. In the dominant one, there is a S−C_2 bond and the unpaired electron is centered on C_4, which is not bonded to sulfur; in the other structure, the terminal carbon atoms switch their roles.

III.2. Transition States. The transition state for the M2 ↔ M1 isomerization is TS12. The analysis of the normal mode of imaginary frequency indicates that the carbon atom bonded to sulfur in M1 will be C_2, in other words, the S−C_3 bond of M2 disappears when this species transforms into M1. It must be noted that we could not find a minimum with a SC_2 cycle, apart from M6.

The isomerization of M2 into M3 takes place through the transition state TS23. This process involves migration of hydrogen to the carbon atom bonded to sulfur and simultaneous opening of the C_3 cycle.

M3 is connected to M4 through the saddle point TS34; this process is simply a carbon-to-sulfur hydrogen migration, which takes place in the molecular plane. M4 may isomerize into the other thiol, M5, by simple migration of the terminal carbon atom through TS45. On the other hand, M3 may also evolve into M6, through transition structure TS36. M6 may rearrange into M7 through TS67; this process would involve breaking of the C_2−C_4 bond of M6 and formation of a C_2−C_5 linkage. M8 may isomerize into M2 through TS28 or into M7 through TS78. The former transition state is not very high in energy; in fact, it lies only 7.4 kcal/mol above M8; TS78 however is very much higher in energy.

We also located structure TS19, which corresponds to the M9 ↔ M1 isomerization. This process would involve hydrogen migration to a terminal carbon of M9 and subsequent breaking of the SC_3 cycle.

We also found saddle points TS1H, TS3H, and TS4H for the hydrogen elimination process from M1, M3, and M4, respectively.

The generation of SC + C_2H or S + *l*-C_3H from M1 or S + *c*-C_3H from M2 do not appear to have saddle points. At least, we made potential surface scans at the QCISD/6-31G** level for all of these processes and did not find any indication of the existence of saddle points. We also performed QCISD/6-31G** potential surface scans for hydrogen elimination from M6 and M7 and M8; the corresponding energy profiles correlate with excited states of SC_3,[33] the reaction not being exothermic.

III.3. Local Minima and Transition States on the Quartet PES. Although the quartet−doublet energy gaps computed on the geometries of the doublet local minima are positive and quite wide, we have also determined some local minima on the lowest quartet state. The corresponding geometries are depicted in Figure 2a. The lowest-lying quartet species is M1Q, which lies 56.6 kcal/mol above the corresponding doublet-state minimum M1; the only doublet species lying above M1Q are M6, M7, and M9. The electronic state is $^4A'$, and the leading electron configuration is [...3a″^{1}15a′^{1}4a″^{1}]. We have also performed a partial C_s-constrained optimization of a $^4A''$ species; this electronic state is very close in energy to the $^4A'$ state for the C_s-constrained minimum is in fact −0.2 kcal/mol below M1Q, but we could not achieve convergence for the QCISD/6-311+G(3df,2p) wave function in this case. The other quartet species are all well above M1Q and all doublet species except for M9. M2Q lies 73.1 kcal/mol above M2, whereas M3Q is 39.2 kcal/mol higher in energy than M3. The leading electron configuration of M3Q is [. .14a′^{1}15a′^{1}4a″^{1}] and corresponds to a $^4A''$ state. There is a $^4A'$ state lying very close to $^4A''$; we could locate a $^4A'$ minimum in a C_s-constrained optimization which is only 8.5 kcal/mol higher in energy than M3Q. M4Q has a $^4A'$ electronic state with the dominant electron configuration [...3a″^{1}15a′^{1} 4a″^{1}] and is 43.5 kcal/mol higher in energy than M4.

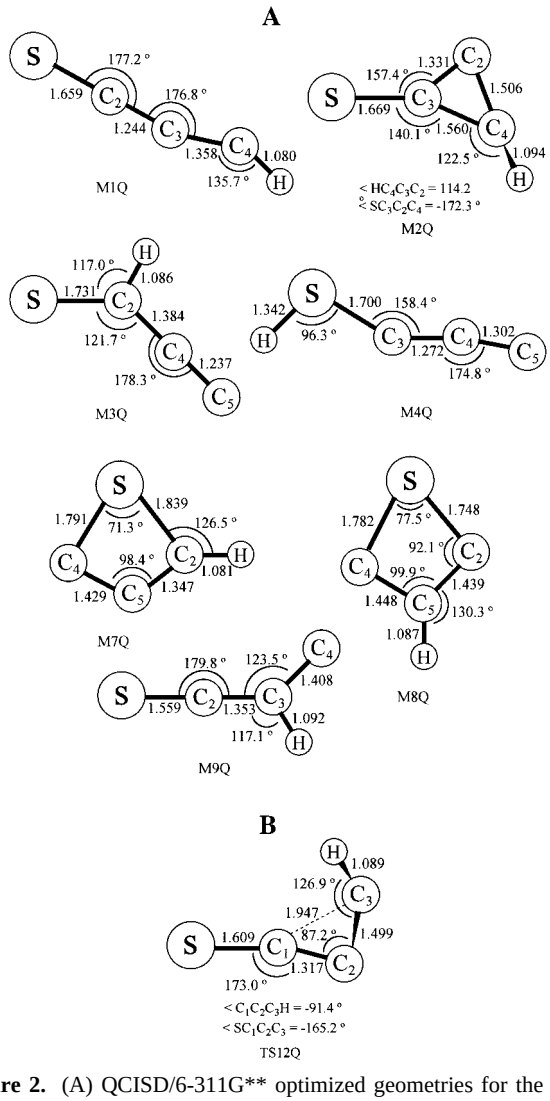

Figure 2. (A) QCISD/6-311G** optimized geometries for the most relevant local minima on the lowest quartet state. (B) QCISD/6-311G** optimized geometry for the transition structure connecting M1Q and M2Q.

We could not find any quartet minima that would correspond to M5 or M6; the B3LYP/6-311G** optimizations give C_3 + SH and M7Q, respectively. M7Q is planar, unlike its doublet counterpart; its electronic state is $^4A''$, and the leading electron configuration is [..14a′^{1}15a′^{1}4a″^{1}]. It lies 25.4 kcal/mol above M7. M8Q lies 44.0 kcal/mol higher in energy than its doublet counterpart; it has a $^4A'$ state with a leading electron configuration of [...3a″^{1}15a′^{1}4a″^{1}]. We could not fully optimize a local minima corresponding to M9 on the quartet surface; a partial optimization constrained to C_s symmetry gave a $^4A''$ state lying 46.4 kcal/mol above M9 at the B3LYP/6-311G** level. We could not locate a structure similar to M10Q on the lowest doublet surface, for all optimizations led to the linear form. The electronic state of M10Q is $^4A''$, and the leading configuration is [...4a″^{1}14a′^{1}15a′^{1}]. It is interesting that all quartet minima except M1Q are rather close in energy.

As we will discuss below, we have not found exothermic reaction channels on the lowest quartet PES, so the only possible process other than dissociation into the reactants should be S + *l*-C_3H → S + *c*-C_3H. Thus, the transition structure linking

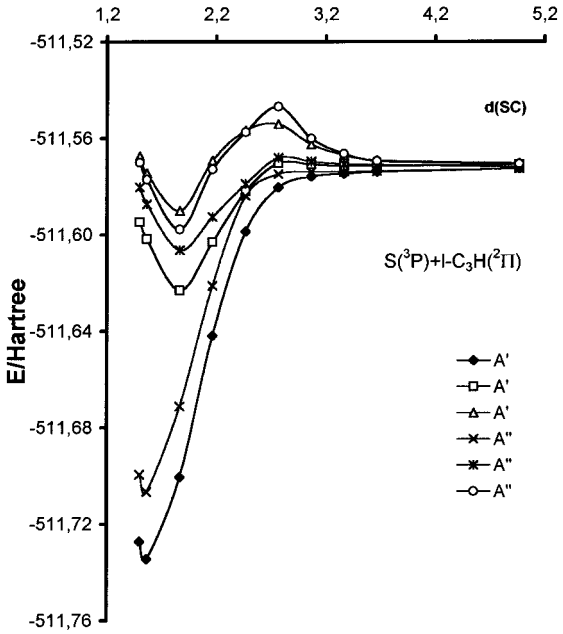

Figure 3. CASSCF/cc-pVDZ energy profiles of the doublet electronic states for the interaction of S(^{3}P) with *l*-C_3H($^2\Pi$).

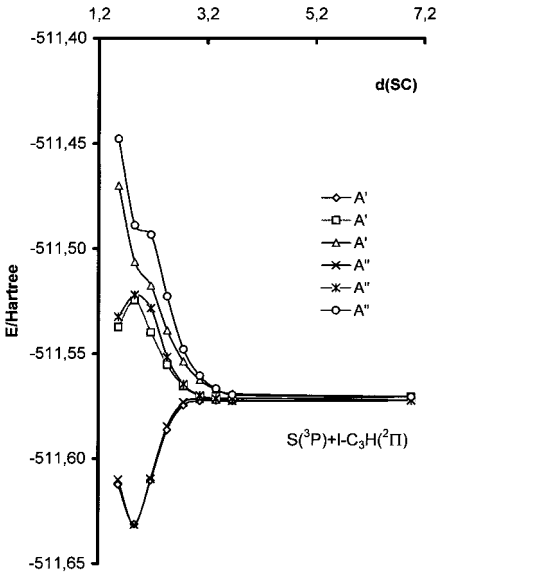

Figure 4. CASSCF/cc-pVDZ energy profiles of the quartet electronic states for the interaction of S(^{3}P) with *l*-C_3H($^2\Pi$).

M1Q and M2Q is relevant, and it will be noted TS12Q and is shown in Figure 2b.

III.4. Energy Profiles. In addition to the QCISD/6-31G** potential surface scans, we computed the energy profiles of the lowest lying states for the interaction between reactants, i.e., for the S + *l*-C_3H and S + *c*-C_3H interactions. The set of geometries employed correspond to the QCISD/6-31G** scans, which were made on the lowest lying ^{2}A′ state for both interactions. In the case of the S + *l*-C_3H interaction (doublet states), we performed state-averaged CASSCF/cc-pVDZ[28,35] computations for every point including three ^{2}A′ states and also three ^{2}A″ states, which correlate all with the ground-state reactants S(^{3}P) + C_3H($^2\Pi$). The active space was [12a′−18a′, 2a″−5a″] for eleven electrons. For the quartet states, we used the same active space and included three states of both the ^{4}A′ and ^{4}A″ symmetries in the CASSCF/cc-pVDZ computation. In the case of the S + *c*-C_3H interaction (doublet states), we did the same but including nine ^{2}A′ states and eight ^{2}A″ states and the following active space [11a′−17a′, 3a″−5a″] for 11 electrons. For the quartet states, we used as active space [11a′−17a′, 3a″−4a″] and included two ^{4}A′ states and four ^{4}A″ states in the CASSCF/cc-pVDZ computation. The resulting energy profiles are shown in Figures 3−7.

It is readily seen in Figure 3, which belongs to the interaction between S and *l*-C_3H, that there are two neatly repulsive potential surfaces corresponding to the highest lying ^{2}A′ and ^{2}A″ electronic states. Even though one must not forget that the set of molecular geometries correspond to the lowest ^{2}A′ state, the barriers are high enough to conclude that both potential surfaces could indeed be repulsive. The case of the two states having small barriers is quite different, for they might well disappear if a true reaction coordinate were used or even if the dynamical correlation effects not captured by the CASSCF wave functions were included. It is clear though, that there are a couple of neatly attractive doublet potential surfaces. Concerning the behavior of the quartet states (Figure 4), it is readily seen that they are all repulsive except for the lowest ^{4}A′ and ^{4}A″ states.

The energy profiles of the S + *c*-C_3H reaction are more complex because of the strong interaction between many low-lying electronic states including avoided crossings and the effects

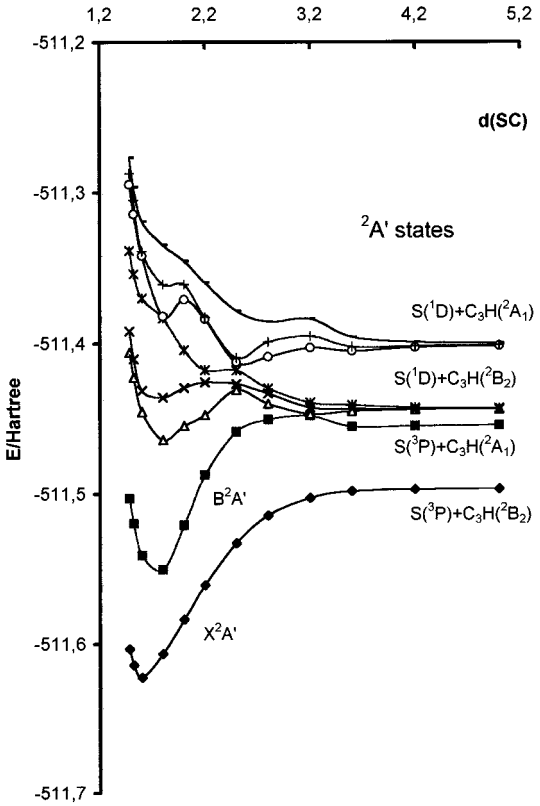

Figure 5. CASSCF/cc-pVDZ energy profiles of the doublet electronic states (^{2}A′) for the interaction of S(^{3}P,^{1}D) with *c*-C_3H($^2B_2$,$^2A_1$).

of the geometrical distortion of the *c*-C_3H group along the reaction coordinate. It must be stressed that one must take into account a very low lying excited state of *c*-C_3H, namely, $^2A_1$, for it might have some influence in the reaction dynamics as we will show immediately. It has already been established that this state becomes even lower in energy than the ground state ($^2B_2$) upon a quite small variation of the <HCC angle (about 5°)[36] and that the energy changes involved are comparable to the S(^{3}P)−S(^{1}D) energy gap. Both states of *c*-C_3H correlate with ^{2}A′ states of planar geometries, so S(^{3}P) + *c*-C_3H($^2B_2$,$^2A_1$) gives rise to two ^{2}A′ and four ^{2}A″ states (quartet states are not included). It is readily seen in Figures 5 and 6 that both ^{2}A′

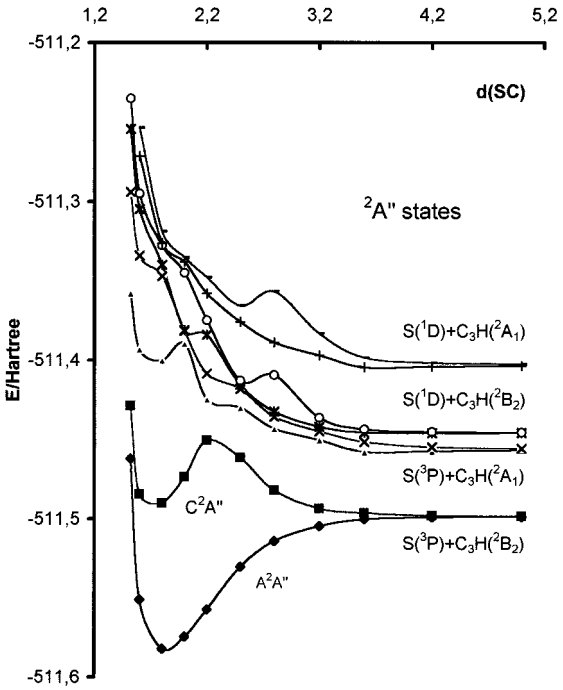

Figure 6. CASSCF/cc-pVDZ energy profiles of the doublet electronic states (^{2}A″) for the interaction of S(^{3}P,^{1}D) with *c*-C$_3$H(^{2}B$_2$,^{2}A$_1$).

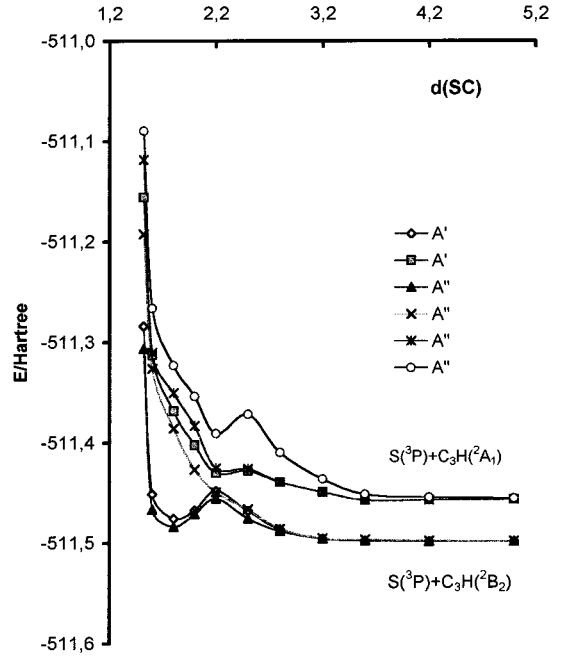

Figure 7. CASSCF/cc-pVDZ energy profiles of the quartet electronic states for the interaction of S(^{3}P)+*c*-C$_3$H(^{2}B$_2$) with S(^{3}P)+*c*-C$_3$H(^{2}A$_1$).

states are attractive while only the lowest ^{2}A″ state is attractive. The other ^{2}A″ state which correlates with the ground-state reactants (C^{2}A″) increases its energy quite steeply with decreasing S−C distance and presents a maximum at *d*(SC) ≈ 2.2 Å, mainly as a result of the repulsion of a p-electron pair of sulfur located along the S−C bond axis. One encounters the same behavior in the case of the pairs of ^{2}A″ states that correlate with S(^{1}D) + *c*-C$_3$H(^{2}B$_2$,^{2}A$_1$), although not for the one correlating with S(^{3}P) + *c*-C$_3$H(^{2}A$_1$), probably because of the interaction with the lowest component of the pair that correlates with S(^{1}D) + *c*-C$_3$H(^{2}B$_2$). Note there is an intersection between the C^{2}A″ and B^{2}A′ states; it is quite high in energy according to our computations, but geometrical and electron correlation effects may strongly affect its location, so we would not discard it may have some influence on the dynamics of the S(^{3}P) + *c*-C$_3$H(^{2}B$_2$) reaction. In any case, it certainly provides a reaction path for the interaction between S(^{3}P) and *c*-C$_3$H(^{2}A$_1$); the barrier of the B^{2}A′ profile appears to be quite small. It must also be pointed out this barrier is caused by an avoided crossing between the B^{2}A′ state and the lowest of the group which correlates with S(^{1}D) + *c*-C$_3$H(^{2}B$_2$), so collisions between these two radicals may be reactive as well by virtue of this feature.

According to Figure 7, the quartet states are repulsive; however, the lowest two states present relatively low barriers. We could locate a transition state for the elimination of sulfur from M2Q at the QCISD/6-31G** and QCISD/6-311G** levels (the S−C distance was 2.568 Å in the latter case, and the imaginary frequency only 128i cm^{-1} at the QCISD/6-31G** level). All attempts to locate it at B3LYP levels led to S + *c*-C$_3$H. However, this transition structure actually lies 1.6 kcal/mol *lower* in energy than S + cC$_3$H(^{2}B$_2$) at the QCISD(T)/6-311+G(3df,2p)//QCISD/6-311G**+ZPVE(QCISD/6-31G**) level, so it is doubtful that there really exists an energy barrier for the generation of M2Q from sulfur and *c*-C$_3$H on the lowest quartet state; the latter energy difference is so small that very high level computations would be required to provide a definitive assessment of this point. Even if the lowest two quartet PES are attractive, the importance of quartet states in the reaction dynamics would also depend on the efficiency of the nonadiabatic processes leading to the attractive doublet states (see also next section).

III.5. Reaction Paths. The reaction of S with *l*-C$_3$H or *c*-C$_3$H is exothermic for the generation of SC($^1\Sigma^+$) + C$_2$H($^2\Sigma^+$) and SC$_3$($^1\Sigma^+$) + H(^{2}S). The results of a study of the excited states of SC$_3$[33] indicate that none of them can be formed in these reactions for the reaction would be endothermic, although at least the lowest-lying excited state of C$_2$H ($^2\Pi$ in linear geometries) could be formed.[37] There are basically two types of reaction paths, one involves the ground state of the SC$_3$H system (M1) and the other involves several other intermediates. For simplicity, we do not include in the following reaction schemes the highest lying minima, i.e., (M5 to M9):

$$\text{S} + c\text{-C}_3\text{H} \rightarrow \text{M2} - \text{TS12} \rightarrow \text{M1} - \text{TS1H} \rightarrow \text{SC}_3(^1\Sigma^+) + \text{H} \quad (1a)$$

$$\text{S} + c\text{-C}_3\text{H} \rightarrow \text{M2} - \text{TS12} \rightarrow \text{M1} \rightarrow \text{SC}(^1\Sigma^+) + \text{C}_2\text{H}(^2\Sigma^+) \quad (2a)$$

$$\text{S} + c\text{-C}_3\text{H} \rightarrow \text{M2} - \text{TS23} \rightarrow \text{M3} - \text{TS3H} \rightarrow \text{SC}_3(^1\Sigma^+) + \text{H} \quad (3a)$$

$$\text{S} + c\text{-C}_3\text{H} \rightarrow \text{M2} - \text{TS23} \rightarrow \text{M3} - \text{TS34} \rightarrow \text{M4} - \text{TS4H} \rightarrow \text{SC}_3(^1\Sigma^+) + \text{H} \quad (4a)$$

$$\text{S} + l\text{-C}_3\text{H} \rightarrow \text{M1} - \text{TS1H} \rightarrow \text{SC}_3(^1\Sigma^+) + \text{H} \quad (1b)$$

$$\text{S} + l\text{-C}_3\text{H} \rightarrow \text{M1} \rightarrow \text{SC}(^1\Sigma^+) + \text{C}_2\text{H}(^2\Sigma^+) \quad (2b)$$

$$\text{S} + l\text{-C}_3\text{H} \rightarrow \text{M1} - \text{TS12} \rightarrow \text{M2} - \text{TS23} \rightarrow \text{M3} - \text{TS3H} \rightarrow \text{SC}_3(^1\Sigma^+) + \text{H} \quad (3b)$$

$$\text{S} + l\text{-C}_3\text{H} \rightarrow \text{M1} - \text{TS12} \rightarrow \text{M2} - \text{TS23} \rightarrow \text{M3} - \text{TS34} \rightarrow \text{M4} - \text{TS4H} \rightarrow \text{SC}_3(^1\Sigma^+) + \text{H} \quad (4b)$$

The reactants are in their electronic ground states. The dissociation of the M1 or M2 intermediates should also be taken

into account in any dynamical treatment of the S + C_3H reaction, as well as all possible reverse processes. One of these dissociation processes, M2 → S + *c*-C_3H, makes it possible the overall process to be S + *l*-C_3H → S + *c*-C_3H. However this reaction would hardly be competitive with the isomerization of M2 into M3, for TS23 is much lower in energy than the products. A dynamical study appears to be essential given that all of the saddle points involved in the processes 1a−4b are relatively close in energy. Note that TS1H lies 14.0 kcal/mol below TS12; given that the former transition structure is also less tight than TS12, according to their vibrational frequencies, one would expect mechanism 1b to be the most important leading to $SC_3(^1\Sigma^+)$ + H in the case of the $S(^3P)$ + *l*-C_3H reaction. However, it is difficult to foresee whether the generation of $SC(^1\Sigma^+)$ + $C_2H(^2\Sigma^+)$ from M1 would be competitive, for this process has no saddle point, in other words, it has a loose transition state which should have a larger density of states for a given energy. Note that the products $SC(^1\Sigma^+)$ + $C_2H(^2\Sigma^+)$ are only 11.8 kcal/mol higher in energy than TS1H.

The $S(^3P)$ + *c*-C_3H reaction mechanism might be quite complicated. TS23 is 7.5 kcal/mol lower in energy than TS12; because both structures are similarly tight in nature according to their vibrational frequencies, one would expect M3 to be formed in most of the reaction events. TS3H and TS34 have almost the same energy and are similarly tight, so one would foresee that processes 3a and 4a are both important. It should be made clear that M4 may dissociate into $SC_3(^1\Sigma^+)$ + H through TS4H (process 4a) but also isomerize into M5 through TS45; the latter saddle point is even 0.6 kcal/mol lower in energy than TS4H. However, according to our potential surface scans, hydrogen elimination from M5 entails the opening of the C_3 ring; TS4H can be considered the hydrogen-elimination saddle point for both M4 and M5.

It must also be noted that the reaction $SC(^1\Sigma^+)$ + $C_2H(^2\Sigma^+)$ → $SC_3(^1\Sigma^+)$ + H is exothermic and might proceed through M1 with no activation energy. Any route involving M2 will probably have no impact in the reaction rate for TS12 is 2.2 kcal/mol higher in energy than the reactants.

Finally, there are no exothermic reaction channels on the quartet PES; $SC_3(^3A')$ lies 62.2 kcal/mol above $SC_3(^1\Sigma^+)$,[33] $SC(^3\Pi)$ is 86.7 kcal/mol higher in energy than $SC(^1\Sigma^+)$,[37] and $C_2H(^4A')$ lies 93.6 kcal/mol above $C_2H(^2\Sigma^+)$ (see also Table 1). According to our computations, the process S + *l*-C_3H → M1Q → TS12Q → M2Q → S + *c*-C_3H should be possible, but its impact would depend on the efficiency of the nonadiabatic quartet-doublet transitions.

IV. Conclusions

A theoretical study of the potential surfaces of the S + *c*-C_3H and S + *l*-C_3H reactions has been carried out. We have obtained nine doublet and seven quartet minima, which would be reaction intermediates; some of them have peculiar electronic structures. The lowest lying states are a nearly linear SCCCH chain ($^2A'$) and a $SC_3H(^2A')$ species which has a C_3H group attached to sulfur and is 17.1 kcal/mol higher in energy. The vertical energy gap between the ground and the lowest lying electronic states of each doublet intermediate has also been determined through MRCI computations.

The reaction is exothermic for the generation of $SC_3(^1\Sigma^+)$ + H and $SC(^1\Sigma^+)$ + $C_2H(^2\Sigma^+)$; the zero-point reaction energies being −48.4 and −35.5 kcal/mol, respectively. No excited electronic state of SC_3 can be formed. The possible reaction paths are rather complicated for the products may be generated from $SCCCH(^2A')$ through C−H or C−C bond fission processes, or may involve other intermediates that would undergo C−H or S−H bond breaking steps. We have also computed energy profiles for the interaction of sulfur with *l*-C_3H and *c*-C_3H through the lowest lying doublet and quartet states. There are neatly attractive electronic states in both cases for *l*-C_3H and also for *c*-C_3H in the case of the doublet states.

Our final conclusion is that the S + C_3H reaction could indeed be a source of $SC_3(^1\Sigma^+)$, but its efficiency would depend very much on the SC_3 + H/SC + C_2H branching ratio. Experimental or detailed theoretical dynamical studies are necessary in order to determine the branching ratios, for a qualitative analysis of the potential energy surfaces suggests that generation of both $SC_3(^1\Sigma^+)$ + H and $SC(^1\Sigma^+)$ + $C_2H(^2\Sigma^+)$ might be important processes.

Acknowledgment. We are glad to acknowledge financial support from the government of the autonomous community of Galicia (Projects PGIDT99PXI30102B and PGIDT00PXI30104PN) and the Spanish ministry of education (Project PB98-1085).

References and Notes

(1) Smith, D. *Chem. Rev.* **1992**, *92*, 1473.
(2) Lovas, F. J.; Suenram, R. D.; Ogata, T.; Yamamoto, S. *Astrophys. J.* **1992**, 399, 325.
(3) Ohshima, Y.; Endo, Y. *J. Mol. Spectrosc.* **1992**, *153*, 627.
(4) Hirahara, Y.; Ohshima, Y.; Endo, Y. *Astrophys. J.* **1993**, *408*, L113.
(5) Kasai, Y.; Obi, K.; Ohshima, Y.; Hiahara, Y.; Endo, Y.; Kawaguchi, K.; Murakami, A. *Astrophys. J.* **1993**, 410, L45.
(6) Tang, J.; Saito, S. *J. Mol. Spectrosc.* **1995**, *169*, 92.
(7) Szczepanski, J.; Hodyss, R.; Fuller, J.; Vala, M. *J. Phys. Chem.* **1993**, *97*, 1975.
(8) Maier, G.; Reisenauer, H. P.; Schrot, J.; Janoschek, R. *Angew. Chem. Int. Ed. Engl.* **1990**, *29*, 1464.
(9) Lee, S. *Chem. Phys. Lett.* **1997**, *268*, 69.
(10) Maclagan, R. G. A. R.; Sudkeaw, P. *Chem. Phys. Lett.* **1992**, *194*, 147.
(11) Peeso, D. J.; Ewing, D. W.; Curtis, T. T. *Chem. Phys. Lett.* **1990**, *166*, 307.
(12) Murakami, A. *Astrophys. J.* **1990**, *357*, 288.
(13) Seeger, S.; Botschwina, P.; Flügge, J.; Reisenauer, H. P.; Maier, G. *J. Mol. Struct. (THEOCHEM)* **1994**, *303*, 213.
(14) Millar, T. J.; Flores, J. R.; Markwick, A. J. *Mont. Not. R. Astron. Soc.* **2001**, *327*, 1173.
(15) Petrie, S. *Mont. Not. R. Astron. Soc.* **1996**, *281*, 666.
(16) Turner, B. E.; Lee, H.-H.; Herbst, E. *Astrophys. J. Supp. S.* **1998**, *115*, 91.
(17) Flores, J. R.; Estevez, C. M.; Carballeira, L.; Juste, I. *J. Phys. Chem. A.* **2001**, *105*, 4716.
(18) Becke, A. D. *J. Chem. Phys.* **1993**, *98*, 5648.
(19) Pople, J. A. Head-Gordon, M.; Raghavachari, K. *J. Chem. Phys.* **1987**, *87*, 5968.
(20) McLean, A. D.; Chandler, G. S. *J. Chem. Phys.* **1980**, *72*, 5639.
(21) González, C.; Schlegel, H. B. *J. Chem. Phys.* **1989**, *90*, 2154; *J. Phys. Chem.* **1994**, *94*, 5523.
(22) Curtiss, L. A.; Carpenter, J. E.; Raghavachari, K.; Pople, J. A. *J. Chem. Phys.* **1987**, *87*, 5968.
(23) Chase, M. W., Jr. NIST-JANAF Thermochemical Tables, 4th ed. *J. Phys. Chem. Ref. Data. Monograph* **1998**, *9*, 1−1951; http://webbook.nist.gov.
(24) Curtiss, L. A.; Raghavachari, K.; Trucks, G. W.; Pople, J. A. *J. Chem. Phys.* **1991**, *94*, 7221.
(25) Frisch, M. J.; Trucks, G. W.; Schlegel, H. B.; Gill, P. M. W.; Johnson, B. G.; Robb, M. A.; Cheeseman, J. R.; Keith, T.; Petersson, G. A.; Montgomery, J. A.; Raghavachari, K.; Al-Laham, M. A.; Zakrzewski, V. G.; Ortiz, J. V.; Foresman, J. B.; Cioslowski, J.; Stefanov, B. B.; Nanayakkara, A.; Challacombe, M.; Peng, C. Y.; Ayala, P. Y.; Chen, W.; Wong, M. W.; Andres, J. L.; Replogle, E. S.; Gomperts, R.; Martin, R. L.; Fox, D. J.; Binkley, J. S.; Defrees, D. J.; Baker, J.; Stewart, J. P.; Head-Gordon, M.; Gonzalez, C.; Pople, J. A. *Gaussian 94*; Gaussian, Inc.: Pittsburgh, PA, 1995.
(26) Frisch, M. J.; Trucks, G. W.; Schlegel, H. B.; Scuseria, G. E.; Robb, M. A.; Cheeseman, J. R.; Zakrzewski, V. G.; Montgomery, J. A., Jr.; Stratmann, R. E.; Burant, J. C.; Dapprich, S.; Millam, J. M.; Daniels, A. D.; Kudin, K. N.; Strain, M. C.; Farkas, O.; Tomasi, J.; Barone, V.; Cossi,

M.; Cammi, R.; Mennucci, B.; Pomelli, C.; Adamo, C.; Clifford, S.; Ochterski, J.; Petersson, G. A.; Ayala, P. Y.; Cui, Q.; Morokuma, K.; Malick, D. K.; Rabuck, A. D.; Raghavachari, K.; Foresman, J. B.; Cioslowski, J.; Ortiz, J. V.; Stefanov, B. B.; Liu, G.; Liashenko, A.; Piskorz, P.; Komaromi, I.; Gomperts, R.; Martin, R. L.; Fox, D. J.; Keith, T.; Al-Laham, M. A.; Peng, C. Y.; Nanayakkara, A.; Gonzalez, C.; Challacombe, M.; Gill, P. M. W.; Johnson, B. G.; Chen, W.; Wong, M. W.; Andres, J. L.; Head-Gordon, M.; Replogle, E. S.; Pople, J. A. *Gaussian 98*, revision x.x; Gaussian, Inc.: Pittsburgh, PA, 1998.

(27) Werner H.-J.; Knowles, P. J.; Amos, R. D.; Bernhardsson, A.; Berning, A.; Celani, P.; Cooper, D. L.; Deegan, M. J. O.; Dobbyn, A. J.; Eckert, F.; Hampel, C.; Hetzer, G.; Korona, T.; Lindh, R.; Lloyd, A. W.; McNicholas, S. J.; Manby, F. R.; Meyer, W.; Mura, M. E.; Nicklass, A.; Palmieri, P.; Pitzer, R.; Rauhut, G.; Schütz, M.; Stoll, H.; Stone, A. J.; Tarroni, R.; Thorsteinsson. T. University of Birmingham, 1999; *MOLPRO*; http://www.tc.bham.ac.uk/molpro.

(28) Werner, H.-J. *Adv. Chem. Phys*. **1987**, *LXIX*, 1.

(29) McCarthy, M. C.; Vrtilek, J. M.; Gottlieb, E. W.; Tao, F.-M. Gottlieb, C. A.; Thaddeus, P. *Astrophys. J*. **1994**, *L127-L130*, 431.

(30) Hirahara, Y.; Ohshima, Y.; Endo, Y. *J. Chem. Phys*. **1994**, *101*, 7342.

(31) Knowles, P. J.; Hampel, C.; Werner, H.-J. *J. Chem. Phys*. **1993**, *99*, 5219.

(32) d(SC) = 1.593, d(C_2C_3) = 1.379, d(C_3C_4) = 1.246, d(CH) = 1.080, <SCC = 147.8, <$C_2C_3C_4$ = 171.3, <C_3C_4H = 174.3 (angles defined as in Figure 1a).

(33) Flores, J. R.; Pérez Juste, I.; Carballeira, L.; Estévez, C.; Gómez, F. *Chem. Phys. Lett*. **2001**, *343*, 105.

(34) Feller, D.; Huyser, E-.S.; Borden, W. T.; Davidson, E. R. *J. Am. Chem. Soc*. **1983**, *105* 1459.

(35) Woon, D. E.; Dunning, T. H., Jr. *J. Chem. Phys*. **1993**, *98*, 1358.

(36) Yamagishi, H.; Taiko, H.; Shimagawara, S.; Murakami, A.; Noro, T.; Tanaka, K. *Chem. Phys. Lett*. **1996**, *250*, 165.

(37) Jacox, M. E. Vibrational and Electronic Energy Levels of Polyatomic Transient Molecules. In *NIST Chemistry WebBook, NIST Standard Reference Database Number 69*; Mallard, W. G., Linstrom, P. J., Eds.; National Institute of Standards and Technology: Gaithersburg MD, 2000; http://webbook.nist.gov.